03,13

Study of Si(100) surface step convergence kinetics

© M.Yu. Yesin, A.S. Deryabin, A.V. Kolesnikov, A.I. Nikiforov

Rzhanov Institute of Semiconductor Physics, Siberian Branch, Russian Academy of Sciences, Novosibirsk, Russia

E-mail: yesinm@isp.nsc.ru

Received September 11, 2022
Revised October 26, 2022
Accepted November 18, 2022

In this work, the convergence kinetics investigations of the S_A- and S_B-steps on Si(100) substrates with inclination 0.5° and 0.1° were carried out. Analysis of the time dependence of reflection high-energy electron diffraction (RHEED) intensity was used to establish the growth kinetics character on vicinal Si(100) surfaces. It is shown that, in a Si flow at the growth rate of 0.37 ML/s, the step convergence velocity has a decreasing exponential dependence with the temperature increase. It is determined that the single-domain surface formation velocity increases with an increase in the terrace width on the surface, which may be due to the partial participation of growth due to the formation of two-dimensional islands. Above a temperature of 650°C, the dominant growth mode is due to the step movement and the single-domain surface formation velocity decreases with an increase in the terrace width. Thus, the single-layer step convergence is determined by both the MBE growth conditions and the Si(100) substrate orientation. The convergence of S_A- and S_B-steps of the Si(100) surface is explained by the slowdown of the step S_A-motion, which is associated with complex permeability mechanisms and a kink formation of steps. It is assumed that the reason for the slowdown of the step convergence with increasing temperature is an increase in the kink density at the S_A-step, which reduces the step S_A-permeability coefficient.

Keywords:: Molecular-beam epitaxy, reflection high-energy electron diffraction, surface, terraces, steps, kinks.

DOI: 10.21883/PSS.2023.02.55397.476

1. Introduction

Phase diagram of vicinal Si(001) surface showing stability regions of single- and double-layer steps was calculated in early days [1]. Stepped Si(001) surface with single- and double-layer steps will be formed at certain miscut angles and temperatures of the Si(001) substrate. The Si(001) substrate with a miscut angle less than 2.5° is characterized by two-domain surface with monoatomic steps [2]. With certain temperatures of the surface and a certain growth rate, the surface with monoatomic steps will transit to the surface with doubled steps. Previously it was shown [3–5], that in the region of relatively low temperatures a single-domain surface is formed, while in the region of high temperatures a wo-domain surface is formed. The kinetics of monolayer steps doubling into bilayer steps was previously investigated by authors of [6], where the main attention was paid to the misorientation of Si(100) plates at miscut angles of 0.5−4° toward the [110] azimuth. In [7], the doubling of steps was investigated in the temperature range of 450−550°C. In our study we have investigated step convergence in the temperature range of 450−700°C on Si(100) substrates with miscut angles of 0.5 and 0.1°.

The applicability of these investigations consists in that quality of epitaxial layers of the III−V (A_3B_5) group of semiconductor materials on silicon depends on the orientation of domains in the terrace of the stepped surface of Si(100) substrates and height of the steps [8–10]. This study is focused on the formation of single-domain structure with doubled steps on Si(100) substrates with a small miscut of up to 0.5°, for subsequent growth of A_3B_5/Si(100) type heterostructures.

Fig. 1 shows schematically a stepped surface and a pattern of the RHEED (reflection high-energy electron diffraction). The Si(100) surface with a miscut angle less than 2.5° is a set of terraces separated by monoatomic steps [2]. The direction of dimer rows changes alternately on each terrace. With a Si(100) surface miscut from the {100} plane toward {111} plane strictly around the axis of ⟨110⟩, one of steps will be positioned normally to dimer rows of the top terrace (S_B-step), while another step will be parallel to dimer rows of the top terrace (S_A-step) [11,12]. Due to these structural features the S_A-step is smooth, and the S_B-step is rough [13]. The diffusion toward the steps at T_A- and T_B-terraces is different [12]. This leads to the situation when the concentration of adatoms on the T_A-terrace is higher than that on the T_B-terrace. It can be assumed that in the process of growth the concentrations of adatoms on S_A- and S_B-steps will be different as well. This is related to the fact that the concentration of kinks on S_B-steps is higher than that on S_A-steps [13]. Therefore, larger quantities of adsorbed atoms are accumulated on S_A-steps than on S_B-steps. Thus, a system composed of alternating monoatomic S_A- and S_B-steps on a Si(100) surface is interesting for studying of the kinetics of elementary processes.

Fig. 2 shows terrace width as a function of surface miscut angle. This function is plotted on the basis of trigonometric

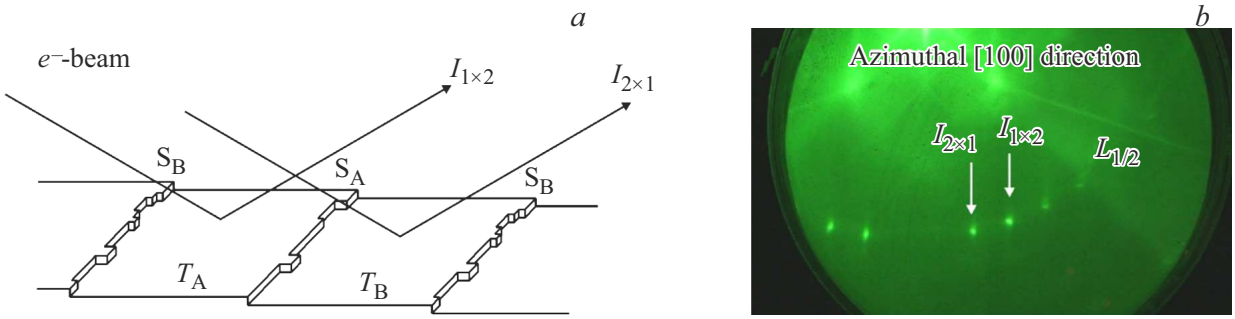

Figure 1. *a* — schematic illustration of a stepped surface and an electron beam, *b* — RHEED pattern from the Si(100) stepped surface.

formulae. With decrease in the miscut angle the terrace width increases as it is shown in Fig. 2. In this study we used Si(100) substrates with miscuts of 0.5 and 0.1°. Terrace widths for Si(100) substrates with miscuts of 0.5 and 0.1° with monoatomic steps are approximately equal to 16 and 78 nm, and terrace widths for biatomic steps are 32 and 156 nm, respectively.

In the equilibrium state the steps are evenly spaced due to the elastic and effective entropic interaction [2,14–17]. However, in the process of molecular-beam epitaxy (MBE) growth of Si on Si(100) a convergence of S_A- and S_B-steps takes place [18]. The step convergence is caused by the presence of both the conventional and inverse Ehrlich–Schwoebel barriers for adatoms attachment to the edge of the S_A-step [19,20]. In [21] it is shown that permeability of the S_A-step promotes faster convergence of S_A- and S_B-steps. In [22], the authors theoretically investigated mechanisms of the step permeability with the use of a simple model of atomic events at the step edge. In the same study [22] it is found that formation of non-equilibrium kinks (the 1D-islands at the step edge) can result in the non-monotonous temperature dependence of the step permeability. Key parameters of the system that takes into account step permeability and kinetic coefficients of adatom incorporation to the step become the following: density of kinks, energy barriers of the step, and diffusion of adatoms at the step edge [23–25]. Also, as it is shown in [26], there is an interaction between kinks. It is shown with the use of simulation, that thermal coarsening of some steps on a Si(100) surface can be interpreted in the best way taking into account the interaction between kinks in the effective Hamiltonian [26]. Thus, the formation of kinks in the process of growth has an effect on the permeability of steps.

The effect of step convergence was not studied experimentally at temperatures higher 550°C. In this context, in this work an attention is paid to the step convergence in the process of MBE growth of Si on Si(100) in the temperature range of 450–700°C, which is wider than that for the previously obtained results known from the literature.

The goal of this study is to determine the effect of conditions of the MBE growth of Si and orientation of

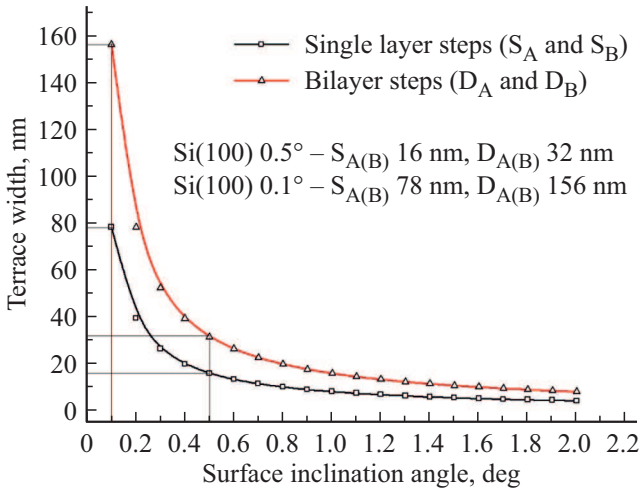

Figure 2. Terrace width as a function of surface miscut angle.

Si(100) substrate on the process of surface step convergence. To achieve this goal, the following tasks were performed: analysis of time dependencies of RHEED reflection intensities $I_{2\times1}$ and $I_{1\times2}$; measurement of the number of deposited Si monolayers at which the surface step convergence takes place at different temperatures on Si(100) substrates with miscut angles of 0.5 and 0.1°.

2. Experimental procedure

The growth was implemented in a „Katun-S“ MBE setup equipped with an electron-beam evaporator for Si. The analytical part of the chamber is composed of a quadrupole mass-spectrometer, a quartz thickness meter, and a diffractometer of fast electrons with an energy of 20 keV. The results are obtained in different process cycles on Si substrates with the same crystal-lattice orientations. The growth was implemented in a flux of Si atoms with a growth rate of 0.37 ML/s (after the shutter opening). We used Si(100) *n*-type substrates with a resistance of 5–10 Ω · cm that had 0.5 and 0.1° miscut off the {100} plane toward the {111} plane strictly around the ⟨110⟩ axis. RHEED patterns were recorded in the [100] azimuth

direction. We analyzed intensities of the reflections located on the fractional-order Laue zone. Change in the RHEED pattern was recorded by video camera. To achieve stationary conditions of the growth, the diffraction patterns were recorded after a period of time required for the thermocouple readings stop changing after a change in the conditions of silicon atoms depositing.

After the procedure of Si(100) surface preparation in an ultrahigh-vacuum chamber (removal of chemical oxide by annealing at 800°C in a flux of silicon atoms of 10^{13} atom/cm^2/s and growth of a 50 nm buffer layer of Si), the substrate was annealed at a temperature of 900°C for 40 min (without the Si atoms flux) [27]. Then the substrate temperature was decreased evenly. In the substrate temperature range of 450–700°C and a Si atoms flux with a growth rate of 0.37 ML/s the intensities of superstructure reflections were measured with open shutter.

According to [28–30], under certain conditions of diffraction a constructive or destructive interference is realized. Electrons scattered by atoms with a distance of r between them can interfere constructively or destructively depending on the wavefunction phase shift between points [29,31], which results in the situation when either the delta function term or the pair correlation function term will be predominant in the beam intensity expression depending on incident and reflection angles of the electron beam [29]. As it is shown in [32,33], the dependence of beam intensity on main parameters of the new growing phase is different in case of predominance of the delta function term or the pair correlation function term. Parameters that describe the beam intensity can be the number of scatterers N, the size of two-dimensional objects L, and the occupancy θ. Due to the low resolution and interpretation complexity of RHEED, it may be difficult to determine precisely the dependence of beam intensity on the main parameters. Therefore, the analysis of RHEED intensity, perhaps, does not reproduce to the full possible extent the surface state. In our study we have initially selected the diffraction conditions with the maximum beam intensity and rounded shape of the beam with the smallest size. The study is carried out in an attempt to reproduce the conditions of growth and diffraction close to those in [7]. Values were determined for the stationary condition. Following the study of [32], our study assumes a direct dependence of the intensity on the number of scatterers and a quadratic dependence on the size of 2D-islands.

3. Results

Fig. 3 shows RHEED reflection intensities $I_{2\times1}$ and $I_{1\times2}$ as functions of time after the shutter opening (in the flux of Si atoms) for the Si(100) substrate with a miscut of 0.5°. The growth was implemented in a flux of Si atoms with a growth rate of 0.37 ML/s (after the shutter opening) and a substrate temperature of 600°C. After the shutter opening, the intensity $I_{2\times1}$ increases, while $I_{1\times2}$ decreases.

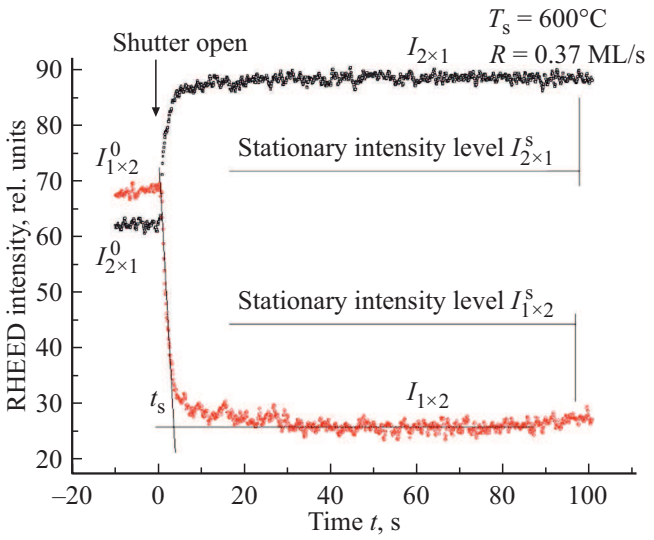

Figure 3. RHEED reflection intensities $I_{2\times1}$ and $I_{1\times2}$ as functions of time.

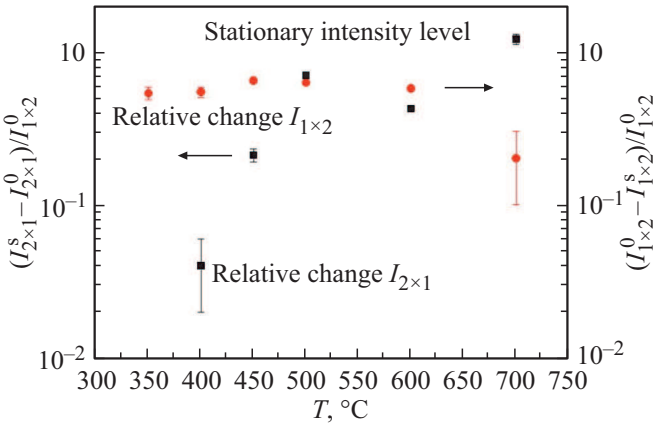

Figure 4. Temperature dependencies of the relative change in intensities $(I^s_{2\times1}-I^0_{2\times1})/I^0_{2\times1}$ and $(I^0_{1\times2}-I^s_{1\times2})/I^0_{1\times2}$ after they have achieved a stationary level.

The dependencies of $I_{2\times1}$ and $I_{1\times2}$ on time have the shape of saturation curves. The maximum step convergence takes place upon achievement of the stationary level of $I_{2\times1}$ and $I_{1\times2}$ curves. In Fig. 3 the initial intensities before the shutter opening (without the silicon atoms flux) $I^0_{2\times1}$ and $I^0_{1\times2}$ are indicated together with the time to achieve the stationary level of intensity t_s, stationary level of intensity $I^s_{2\times1}$ and $I^s_{1\times2}$, and actual intensities of superstructural reflections $I_{2\times1}$ and $I_{1\times2}$.

Fig. 4 shows dependencies of the relative change in the intensity $(I^s_{2\times1}-I^0_{2\times1})/I^0_{2\times1}$ and $(I^0_{1\times2}-I^s_{1\times2})/I^0_{1\times2}$ on the substrate temperature after they have achieved a stationary level. The graph is plotted on the basis of the data for Si(100) substrates with a miscut of 0.5°. The stationary level of $(I^0_{1\times2}-I^s_{1\times2})/I^0_{1\times2}$ is weakly dependent on temperature in the range of 350–600°C and starts decreasing at a temperature above 600°C. The temperature dependence of

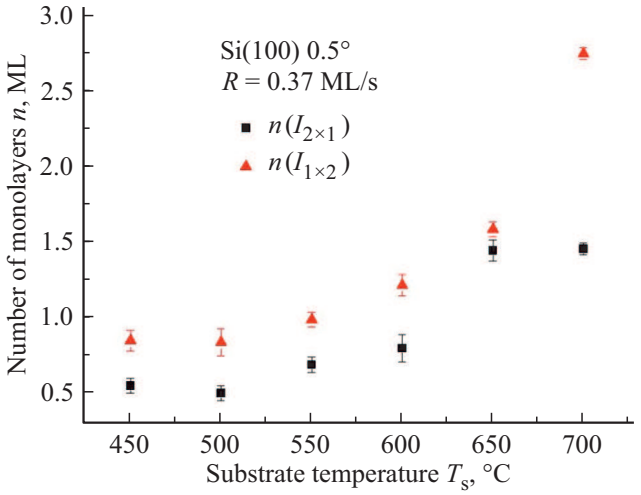

Figure 5. The number of deposited monolayers at which the step convergence occurs as a function of temperature of the Si(100) substrate for a miscut of 0.5°.

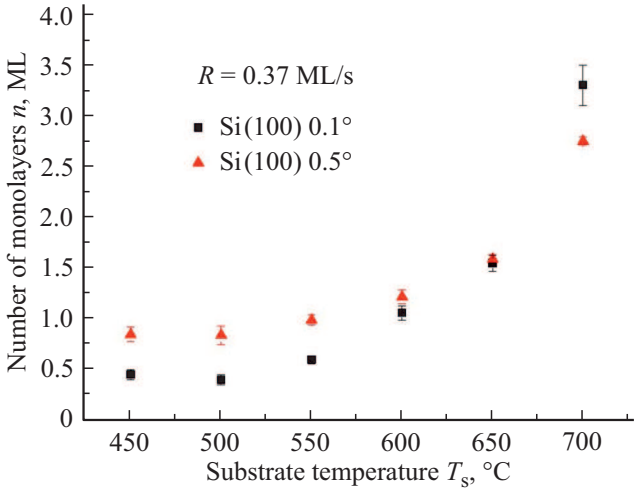

Figure 6. The number of deposited monolayers at which the step convergence occurs as a function of temperature of the Si(100) substrate for miscuts of 0.5 and 0.1°.

$(I^s_{2\times1} - I^0_{2\times1})/I^0_{2\times1}$ in the temperature range of 400–700°C demonstrates increasing behavior.

Based on the dependence of the intensity $I_{2\times1}$ and $I_{1\times2}$ on time, the quantity of deposited material was measured. The measurements were conducted by drawing tangent lines to intensity curves $I_{2\times1}$ and $I_{1\times2}$ as functions of time: in the beginning, when $I_{2\times1}$ and $I_{1\times2}$ start to change sharply, and at the moment of stationary level achievement [34–36]. Thickness of the deposited layer was determined by the time of stationary level achievement by the time dependence of the intensity.

Fig. 5 shows dependencies of the number of deposited monolayers at which the step convergence occurs on the temperature of the Si(100) substrate with a miscut of 0.5°. The growth rate of Si was 0.37 ML/s. The number of deposited monolayers was measured by the change in intensities $I_{2\times1}$ and $I_{1\times2}$ individually. Black dots on the graph in Fig. 5 show the number of monolayers $n(I_{2\times1})$, that were measured by the change in intensity $I_{2\times1}$, while red dots show the number of monolayers $n(I_{1\times2})$ that were measured by the change in intensity $I_{1\times2}$. The numbers of monolayers measured on the basis of the time dependence of $I_{2\times1}$ appeared to be less than those measured on the basis of the time dependence of $I_{1\times2}$. The general trend for all curves is an increase in the number of deposited monolayers at which maximum step convergence occurs with increase in the substrate temperature. The curve $n(I_{1\times2})$ has an exponential dependence on the substrate temperature, and the curve $n(I_{2\times1})$ has a growing dependence which is less manifested.

Fig. 6 shows dependencies of the number of deposited monolayers at which the step convergence occurs on the temperature of the Si(100) substrate with a miscut of 0.5 and 0.1°. The growth rate of Si was 0.37 ML/s. Black dots show the number of monolayers measured in the process of growth on Si(100) substrates with a miscut of 0.1°, red dots show this number for Si(100) substrates with a miscut of 0.5°. In both cases for Si(100) substrates with miscuts of 0.5 and 0.1° the number of monolayers was measured on the basis of change in the intensity $I_{1\times2}$. The temperature dependence of the number of monolayers measured on Si(100) substrates with a miscut of 0.1°, in a similar manner to the Si(100) substrate with a miscut of 0.5°, has an exponential behavior. At temperatures below 650°C, the numbers of monolayers for Si(100) 0.1° substrates are less than those for Si(100) 0.5° substrates. At temperatures over 650°C, on the contrary, the numbers of monolayers for Si(100) 0.1° substrates are higher than those for Si(100) 0.5° substrates.

4. Discussion of results

Time dependencies of intensities $I_{2\times1}$ and $I_{1\times2}$ can be either symmetric or asymmetric, depending on the substrate temperature. At temperatures of 500–600°C, time dependencies become approximately symmetric, while at other temperatures they are asymmetric. As shown in Fig. 4, the relative change in $(I^0_{1\times2} - I^s_{1\times2})/I^0_{1\times2}$ at the stationary level is weakly dependent on temperature in the range of 350–600°C and decreases at temperatures over 600°C. A stronger dependence on temperature has the relative change in $(I^s_{2\times1} - I^0_{2\times1})/I^0_{2\times1}$ at the stationary level or near the first maximum. This behavior of intensities is probably related to the diffusion background.

The time dependence of the relative change in $(I^0_{1\times2} - I^s_{1\times2})/I^0_{1\times2}$ at different temperatures has approximately the same stationary level of intensity. This may be related to the fact that along with the growth the width of T_A-terrace decreases and, as a result, it occupies a minimum area on the surface, while the width of T_B-terrace increases. Perhaps, it leads to an increase in point defects such as

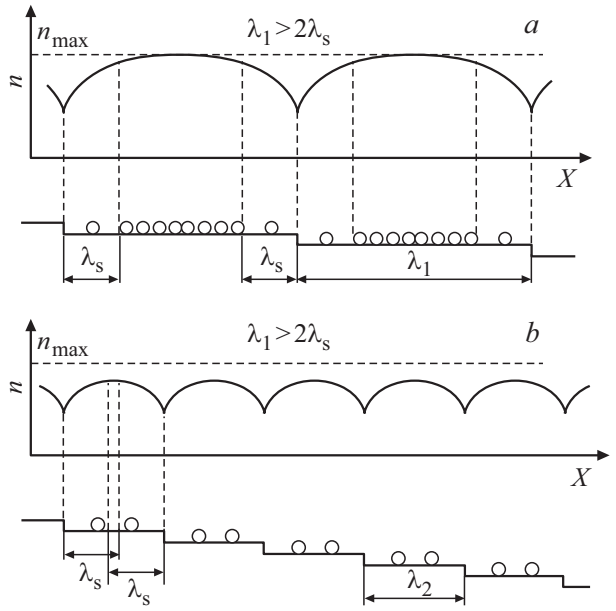

Figure 7. Adsorbed atoms on growing stepped surfaces and curves of their distribution over the surface. Diffusion regions near steps are *a*) not overlapped ($\lambda > 2\lambda_s$), *b*) overlapped ($\lambda < 2\lambda_s$).

adatoms and vacancies on the surface of T_B-terrace, as well as to an increase in the diffusion background [37,38]. Due to the formation of point defects and the increase in diffusion background with temperature decrease, the relative change in $(I^s_{2\times1} - I^0_{2\times1})/I^0_{2\times1}$ at the stationary level decreases. The diffusion scattering, in general, increases if the density of step edges increases, while the intensity of mirror-reflection beam decreases [38].

Causes of the different behavior of intensities $I_{2\times1}$ and $I_{1\times2}$ shown in Fig. 4 and 5 are not clear so far. Perhaps, this difference is related to RHEED features of the kinetics of growth. However, in [7] measurements were only carried out by the time dependence of the decreasing reflection intensity $I_{1\times2}$. In this study, in a similar way to [7], we shall be limited by the analysis of time dependencies of the intensity $I_{1\times2}$.

The growing steps of surface are fed not only (and not so much) by the particles falling on them directly from vapor, but collect the substance from their adjoining surface areas. Atoms and molecules form on the smooth and step-free surface the adsorption gas or liquid in the equilibrium state with the vapor. The substance is delivered to the surface steps by means of surface diffusion. The effect of terrace width on the crystal growth is illustrated in Fig. 7. This figure shows adsorbed atoms on the growing stepped surfaces and curves of their distribution over the surface. *a* — diffusion areas near steps are not overlapped ($\lambda > 2\lambda_s$), *b* — overlapped ($\lambda < 2\lambda_s$). At $\lambda < 2\lambda_s$, the adjacent steps are attract from each other the material delivered from the gas, and the rate of each of them is less than in the case without overlapping. A step can be considered as a continuous linear source or sink for adsorbed particles. In the case of crystal growth this sink absorbs the particles adsorbed on the surface in band with a width of λ_s on both sides of the step, with a predominant probability of re-evaporation [39].

As it is shown on the basis of temperature dependencies of the number of deposited monolayers after the step convergence at temperatures below 650°C, the step convergence occurs faster on Si(100) substrates with wider terraces (Fig. 6). This can be explained by the effect of nucleation of 2D-islands on the T_A-terrace and decrease in the rate of steps motion due to crossing of the diffusion regions. At temperatures over 650°C, the step convergence goes slower on the same substrates. This may be related to the fact that the elastic and effective entropic repulsion between the steps acts stronger.

The speed of step motion is proportional to the number of incorporated adatoms [25,40]. Since the concentration of kinks is high on the S_B-step, the predominant number of adatoms are incorporated in this step. Probably, the S_B-step moves with maximum speed. It is assumed that motion of this step takes place in the mode of limited diffusion growth [21,41,42]. The step convergence occurs due to slowed motion of the S_A-step. A lower number of adatoms are incorporated into the S_A-step as compared with the S_B-step. Perhaps, it happens due to the lower length of diffusion along the step in relation to the distance between kinks, which creates conditions for realization of permeability of the S_A-step. In this case adatoms do not incorporate into kinks and jump over the step, and the step moves slower. The growing temperature dependence of the monolayers number can be explained by the increasing length of adatoms diffusion along the S_A-step.

An alternative explanation of the growing dependence of the deposited monolayers number with temperature is that kinks are formed on the S_A-step. Since the S_A-step contains a considerably lower number of kinks as compared with the S_B-step, growth of the S_A-step requires pre-formation of kinks. Since thermal-activated formation of kinks with a sufficiently high density is slowed down, it is clear that another mechanism should be used [13,41,43–45]. In a similar manner to the formation of 2D-islands on a smooth defect-free surface, 1D-islands can be formed on the step edge. These 1D-islands will be implemented as finite atomic rows and form two kinks. The concentration of adatoms on the step edge will be dependent on the size of the smooth area of the S_A-step. The probability of 1D-islands formation increases in the case of very long section of the S_A-step and a large flux of adatoms to the step. With shorter section of the smooth S_A-step, adatoms will incorporate into kinks by-passing the formation of 1D-islands. Speed of the step will be actually related to the formation and motion of kinks along the step. To make the step moving faster, a number of elementary atomic processes will happen, for example, attachment of adatoms to the step, motion along the step, and incorporation into the kink, while the S_B-step will move due to the direct incorporation of adatoms into kinks on the step.

5. Conclusion

The number of monolayers at step convergence on Si(100) substrates was investigated. It is shown that in a Si flux with a growth rate of 0.37 ML/s the speed of step convergence of a Si(100) surface with miscuts of 0.5 and 0.1° has a decreasing dependence with substrate temperature increase. It is found that the rate of formation of a single-domain surface increases with increase in terrace width on the surface, which, perhaps, is related to the partial participation of the growth due to the formation of 2D-islands. The nucleation of 2D-islands on the T_A-terrace, perhaps, promotes a faster formation of the single-domain surface. The presented results show a nonmonotonous dependence of the step convergence kinetics at temperatures of 450–700°C on Si(100) substrates with miscut angles of 0.5 and 0.1°. At temperatures above 650°C, the predominant growth mode due to steps motion and the rate of single-domain surface formation decrease with increase in width of terraces. This can be explained by the fact that at higher miscut angles of the substrate the elastic interaction between steps is stronger and the transition takes place at higher fluxes. Thus, the convergence speed of single-layer steps in the process of growth is dependent on both the conditions of molecular-beam epitaxy growth and the Si(100) substrate orientation. The convergence of S_A- and S_B-steps of the Si(100) surface is explained by the slowed motion of S_A-steps, which is related to complex mechanisms of permeability and kinks formation on the steps.

Acknowledgments

The authors would like to thank Yu.Yu. Hervieu for the exchange of knowledge, invaluable advices, and interesting ideas.

Funding

This study was supported by the Ministry of Science and Higher Education of the Russian Federation (grant No. 075-15-2020-797 (13.1902.21.0024)).

Conflict of interest

The authors declare that they have no conflict of interest.

References

[1] O.L. Alerhand, A. Nihat Berker, J.D. Joannopoulos, D. Vanderbilt, R.J. Hamers, J.E. Demuth. Phys. Rev. Lett. **64**, *20*, 2406 (1990).
[2] B.S. Swartzentruber, N. Kitamura, M.G. Lagally, M.B. Webb. Phys. Rev. B **47**, *20*, 13432 (1993).
[3] N. Aizaki, T. Tatsumi. Surf. Sci. **174**, *1–3*, 658 (1986).
[4] P.E. Wierenga, J.A. Kubby, J.E. Griffith. Phys. Rev. Lett. **59**, *19*, 2169 (1987).
[5] A.J. Hoeven, J.M. Lenssinck, D. Dijkkamp, E.J. van Loenen, J. Dieleman. Phys. Rev. Lett. **63**, *17*, 1830 (1989).
[6] K. Sakamoto, T. Sakamoto, K. Miki, S. Nagao. J. Electrochem. Soc. **136**, *9*, 2705 (1989).
[7] K. Sakamoto, K. Miki, T. Sakamoto. Thin Solid Films **183**, *1–2*, 229 (1989).
[8] M. Calamiotou, N. Chrysanthakopoulos, Ch. Lioutas, K. Tsagaraki, A. Georgakilas. J. Crystal Growth **227–228**, 98 (2001).
[9] E.A. Emelyanov, D.F. Feklin, M.A. Putyato, B.R. Semyagin, A.K. Gutakovskii, V.A. Seleznev, A.P. Vasilenko, D.S. Abramkin, O.P. Pchelyakov, V.V. Preobrazhenskii, N. Zhicuan, N. Haiqiao. Avtometriya **50**, *3*, 224 (2014).
[10] D.I. Loshkarev, M.O. Petrushkov, D.S. Abramkin, E.A. Emelyanov, M.A. Putyato, A.V. Vasev, M.Yu. Yesin, O.S. Komkov, D.D. Firsov, V.V. Preobrazhenskii. Semiconductors, **54**, *12*, 1548 (2020).
[11] D.J. Chadi. Phys. Rev. Lett. **59**, *15*, 1691 (1987).
[12] Y.-W. Mo, M.G. Lagally. Surf. Sci. **248**, *3*, 313 (1991).
[13] B.S. Swartzentruber, Y.-W. Mo, R. Kariotis, M.G. Lagally, M.B. Webb. Phys. Rev. Lett. **65**, *15*, 1913 (1990).
[14] J. Tersoff, E. Pehlke. Phys. Rev. Lett. **68**, *6*, 816 (1992).
[15] E. Pehlke, J. Tersoff. Phys. Rev. Lett. **67**, *10*, 1290 (1991).
[16] E. Pehlke, J. Tersoff. Phys. Rev. Lett. **67**, *4*, 465 (1991).
[17] T.W. Poon, S. Yip, P.S. Ho, F.F. Abraham. Phys. Rev. Lett. **65**, *17*, 2161 (1990).
[18] W. Hong, Zh. Zhang, Zh. Suo. Phys. Rev. B **74**, *23*, 235318 (2006).
[19] G. Ehrlich, F.G. Hudda. J. Chem. Phys. **44**, *3*, 1039 (1966).
[20] R.L. Schwoebel, E.J. Shipsey. J. Appl. Phys. **37**, *10*, 3682 (1966).
[21] Yu.Yu. Hervieu. Russ. Phys. J. **63**, *6*, 901 (2020).
[22] S.N. Filimonov, Yu.Yu. Hervieu. Surf. Sci. **553**, *1–3*, 133 (2004).
[23] R. Zhao, J.W. Evans, T.J. Oliveira. Phys. Rev. B **93**, *16*, 165411 (2016).
[24] R. Zhao, D.M. Ackerman, J.W. Evans. Phys. Rev. B **91**, *23*, 235441 (2015).
[25] W.K. Burton, N. Cabrera, F.C. Frank. Phil. Trans. R. Soc. Lond. A **243**, *866*, 299 (1951).
[26] Zh. Zhang, Y.-T. Lu, H. Metiu. Surf. Sci. Lett. **259**, *1–2*, L719 (1991).
[27] M.Yu. Yesin, A.I. Nikiforov, A.S. Deryabin, V.A. Timofeev. IEEE Xplore XXI Int. Conf. of Young Specialists on Micro/Nanotechnologies and Electron Devices (EDM), 36 (2020). DOI: 10.1109/EDM49804.2020.9153524
[28] C.S. Lent, P.I. Cohen. Surf. Sci. **139**, *1*, 121 (1984).
[29] P.R. Pukite, C.S. Lent, P.I. Cohen. Surf. Sci. **161**, *1*, 39 (1985).
[30] P.I. Cohen, G.S. Petrich, P.R. Pukite, G.J. Whaley, A.S. Arrott. Surf. Sci. **216**, *1–2*, 222 (1989).
[31] P.R. Pukite. Thesis 188 in partial fulfillment of the PhD requirements. Faculty of the Graduate School, University of Minnesota (1988).
[32] M.C. Tringides, M.G. Lagally. Surf. Sci. **195**, *3*, L159 (1988).
[33] A.V. Vasev, M.A. Putyato, V.V. Preobrazhenskii. Surf. Sci. **677**, 306 (2018).
[34] L. Simon, P. Louis, C. Pirri, D. Aubel, J.L. Bischoff, L. Kubler, D. Bolmont. J. Cryst. Growth **256**, *1–2*, 1 (2003).
[35] V. Le Thanh, V. Yam, N. Meneceur, P. Boucaud, D. Débarre, D. Bouchier. Mater. Phys. Mech. **4**, *2*, 94 (2001).
[36] A.I. Nikiforov, V.A. Timofeev, S.A. Teys, A.K. Gutakovsky, O.P. Pchelyakov. Thin Solid Films **520**, *8*, 3319 (2012).
[37] J.H. Neave, P.J. Dobson, B.A. Joyce, J. Zhang. Appl. Phys. Lett. **47**, *2*, 100 (1985).

[38] P.J. Dobson, B.A. Joyce, J.H. Neave, J. Zhang. J. Cryst. Growth. **81**, *1–4*, 1 (1987).
[39] A.A. Chernov, E.I. Givargizov, Kh.S. Bagdasarov, V.A. Kuznetsov, L.N. Dem'yanets, A.N. Lobachev, Sovremennaya kristallografiya. Nauka, M. (1980). V. 3. 401 p. (in Russian).
[40] S. Stoyanov. Europhys. Lett. **11**, *4*, 361 (1990).
[41] I.V. Markov. Crystal Growth for Beginners: Fundamentals of Nucleation, Crystal Growth and Epitaxy. 2nd ed. World Scientific, Singapore (2003).
[42] Yu.Yu. Hervieu, I. Markov. Surf. Sci. **628**, 76 (2014).
[43] N. Kitamura, B.S. Swartzentruber, M.G. Lagally, M.B. Webb. Phys. Rev. B **48**, *8*, 5704(R) (1993).
[44] B.S. Swartzentruber, M. Schacht. Surf. Sci. **322**, *1–3*, 83 (1995).
[45] M.Yu. Yesin, S.A. Teys,A.I. Nikiforov. J. Surf. Invest.: X-Ray Synchrotron Neutron Tech. 16, 1, 140 (2022)].

Translated by Ego Translating